Author/s:
Shilling, PJ;Bumbak, F;Scott, DJ;Bathgate, RAD;Gooley, PR

Title:
Characterisation of a cell-free synthesised G-protein coupled receptor

Date:
2017-12-01

Citation:
Shilling, P. J., Bumbak, F., Scott, D. J., Bathgate, R. A. D. & Gooley, P. R. (2017). Characterisation of a cell-free synthesised G-protein coupled receptor. Scientific Reports, 7 (1), https://doi.org/10.1038/s41598-017-01227-z.

Persistent Link:
https://hdl.handle.net/11343/259221

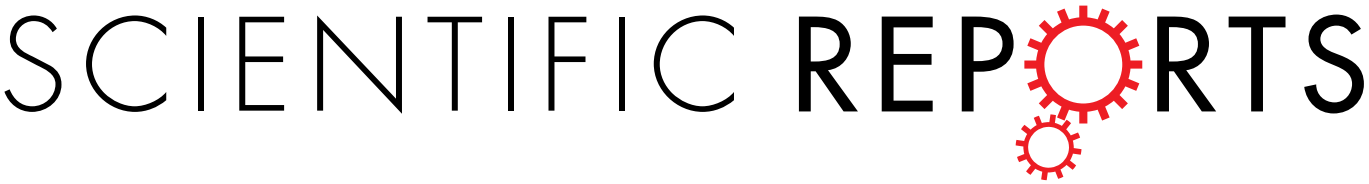

OPEN

Characterisation of a cell-free synthesised G-protein coupled receptor

Received: 21 December 2016
Accepted: 27 March 2017
Published online: 24 April 2017

Patrick J. Shilling[1,2,4], Fabian Bumbak[1,2,3], Daniel J. Scott[1,3], Ross A. D. Bathgate[1,3] & Paul R. Gooley[1,2]

G-protein coupled receptors are the largest family of integral membrane proteins found within the human genome. They function as receptors and modulators to a wide range of ligands and responses which are crucial for human health. GPCR study, specifically the investigation of structure and interaction to cognate ligands, is of high priority. Limitations for structural study can be traced in part, to obtaining suitable quantities of recombinant protein. We sought to address the limitations of traditional recombinant technologies by utilising an *Escherichia coli* based cell-free protein synthesis (CFPS) approach for production of a thermostable neurotensin receptor 1 (en2NTS$_1$). Initial results were promising, with a high amount (up to 2 mg/mL) of en2NTS$_1$ produced, that had attained correct secondary structure. Meanwhile, concurrent experiments indicated that CFPS produced en2NTS$_1$ showed non-competitive binding to the peptide ligand neurotensin8–13 when compared to *E. coli* produced en2NTS$_1$. ^{1}H-^{13}C HMQC SOFAST NMR spectra were indicative of disrupted tertiary structure for CFPS produced $^{13}CH_3$-methionine labelled en2NTS$_1$. The results obtained, indicate CFPS produced en2NTS$_1$ is not forming a discrete tertiary structure and that further development of the CFPS technique needs to be carried out.

G-protein coupled receptors (GPCRs) are a large family of integral membrane proteins of approximately 800 members in humans[1,2]. They constitute the largest group of cell-surface proteins in the human genome and are sorted into four families based on characteristic protein sequences and structural similarity to their prototypical namesake[1]: the rhodopsin family (Class-A), the secretin and adhesion family (Class-B), the glutamate family (Class-C) and the Frizzled/Smoothened family (Class-F)[1,3]. As membrane proteins, GPCRs are the target of many different stimuli that affect a diverse range of responses. Many GPCRs are known to have broad effects on health[4], and therefore, the large number of GPCRs in the human genome may allude to high numbers of possible pharmacological targets for treatment of many ailments. Notably, it has been estimated that 30–40% of all currently marketed pharmaceuticals directly target GPCRs[5]. As a result, the investigation of GPCR structure and function is of high importance.

The characteristic feature shared between all GPCRs is that they possess a transmembrane (TM) domain composed of seven predominantly α-helical transmembrane passes (7TM)[2]. The 7TM helices are arranged in a serpentine pattern in relation to the lipid bilayer and all GPCRs exhibit the same orientation with respect to their insertion into the lipid bilayer: the N-terminus is exposed to the extracellular face of the lipid bilayer and the C-terminal tail projecting into the intracellular space. The individual TM helices are connected by a series of extracellular and intracellular loops. To date, there have been greater than 115 different GPCR structures, of varying conformational states, deposited into the PDB. Most of the successfully obtained GPCR structures have been determined from protein that is produced by recombinant means. The most common expression organisms used for production of GPCRs include insect cells, *Spodoptera frugiperda* or *Trichopulsia ni* and the yeast, *Pichia pastoris*. The main attribute for expression of GPCRs using these organisms, is that they are processed through a similar secretory pathway as in mammalian hosts. Specifically they allow facilitation of receptor folding pathways,

[1]Department of Biochemistry and Molecular Biology, The University of Melbourne, Parkville, VIC, 3010, Australia. [2]Bio21 Molecular Science and Biotechnology Institute, 30 Flemington Road, The University of Melbourne, Parkville, VIC, 3010, Australia. [3]The Florey Institute of Neuroscience and Mental Health, 30 Royal Parade, The University of Melbourne, Parkville, 3052, Victoria, Australia. [4]Present address: Department of Biochemistry and Biophysics, Stockholm University, Stockholm, Sweden. Correspondence and requests for materials should be addressed to P.J.S. (email: patrick.shilling@dbb.su.se) or P.R.G. (email: prg@unimelb.edu.au)

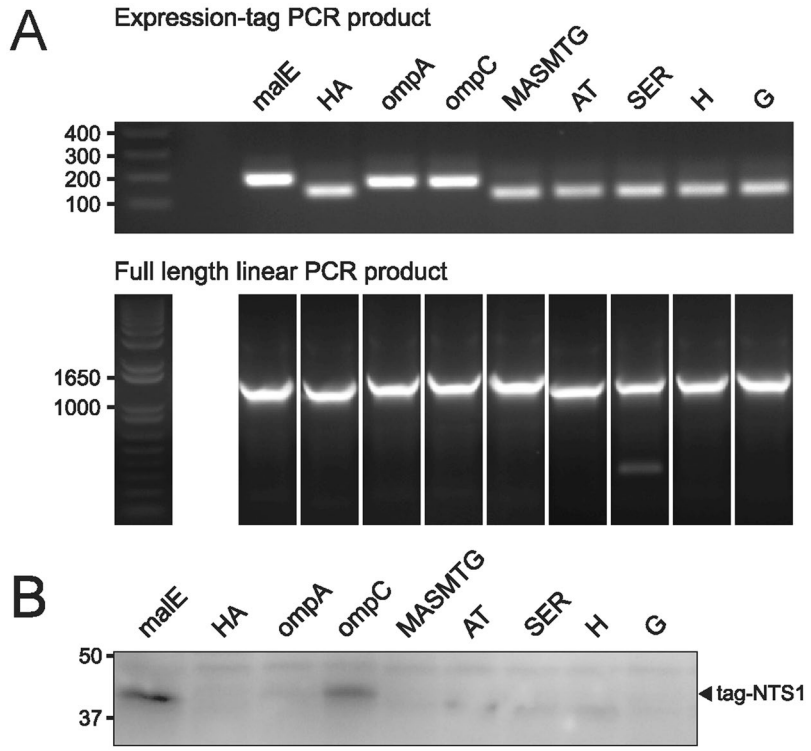

Figure 1. Overlap PCR of linear PCR expression templates and analytical scale CFPS test expression. (**A**) The various expression tags, containing all necessary regulatory elements were generated by an initial PCR. The expression tag, along with the PCR product of en2NTS$_1$ was used to generate the full-length PCR product with the all necessary regulatory elements required for *in vitro* expression. (**B**) Expression was assessed by immunoblot against the His-tag found at the C-terminus of en2NTS$_1$. The malE-signal sequence was identified as the best candidate for expression by CFPS.

protein processing and disulphide bond formation. Additionally, post-translational modifications (PTMs) such as glycosylation may occur, albeit differing in form depending on expression host.

Alternative production techniques for GPCRs include *Escherichia coli* expression or cell-free protein synthesis (CFPS). Expression in *E. coli* is a proven method for expression of some native or mutant GPCRs in a properly folded form that exhibit native ligand binding. Examples include $A_{2A}R$[6], β_1AR[7], CXCR1[8] and NTS$_1$[9,10]. Meanwhile CFPS of folded and functionally active GPCRs has only been successful on a few receptors such as the β_2AR[11], H_1R[12] and dopamine D_2R[13]. Despite limited success, CFPS is a highly sought after technology to produce GPCRs due to the relatively low cost of materials and high yields of protein production. Additionally, CFPS allows the user to directly manipulate and also include unnatural components to the synthesis reaction. The substitution of isotopically labelled or unnatural amino acids makes CFPS a very attractive alternative to traditional recombinant expression. However, expression of membrane proteins by CFPS is challenging, as expression is carried out with minimal or negligible regulation of protein folding. Therefore the operator must supply an environment suitable for solubilisation of the nascent protein or include a refolding step following expression.

Described here is the investigation to assess the functionality and structure of an engineered thermostabilised neurotensin receptor 1 (en2NTS$_1$)[14], produced by CFPS. The work presented demonstrates the capability of CFPS to produce high levels of GPCR protein. The system allowed significant manipulation, by addition of various detergents and replacement of unlabelled methionine with ^{13}C-methyl-methionine for eventual studies of GPCR structure and dynamics by NMR spectroscopy. However ligand binding assays revealed that CFPS produced malE-en2NTS$_1$ showed a propensity to bind non-competitively to the peptide ligand neurotensin8–13 (NT$_{8-13}$). Additionally, NMR studies highlighted that CFPS produced en2NTS$_1$ displayed a non-native tertiary structure, compared to *E. coli* produced en2NTS$_1$, consistent with CFPS producing a poorly folded, non-functional receptor.

Results

en2NTS$_1$ cloning. The first requirement for establishing CFPS production of en2NTS$_1$ was constructing the necessary template for protein synthesis. Based on previous reports which state that reducing mRNA fold at the 5′- end of coding mRNA can lead to optimal likelihood of translation initiation and protein expression[15], we sought to create several N-terminally tagged-based en2NTS$_1$ variants. Creation of the tagged-en2NTS$_1$ variants utilised an overlap PCR approach (Fig. 1A) (Fig. S1 in Supporting Information), whereby nine fusion partners were chosen based on their reported expression enhancement of both soluble and membrane proteins by CFPS[16–18]. The impact of the different expression tags on protein synthesis was performed by analytical scale CFPS expression in the absence of surfactants (precipitate mode CFPS: P-CFPS) so as to allow easy isolation of

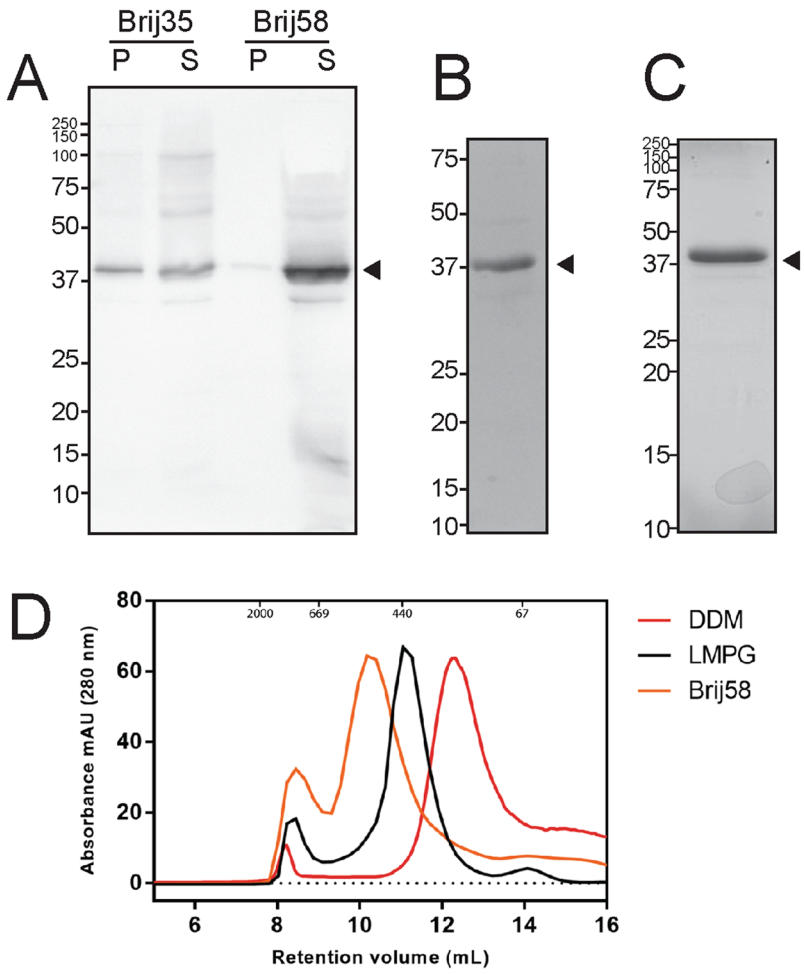

Figure 2. Expression and purification of malE-enNTS$_1$. malE-en2NTS$_1$ could be expressed in either D-CFPS or P-CFPS mode. (**A**) Anti-His immunoblot highlighting better solubility of malE-en2NTS$_1$ in Brij58 compared with Brij35 during D-CFPS mode with near complete solubilisation in the soluble (S) fraction and very little seen in the insoluble pellet (P). (**B** and **C**) Coomassie stained SDS-PAGE of Ni-IMAC purified malE-en2NTS$_1$ obtained from D-CFPS and P-CFPS modes respectively. Arrows indicate malE-en2NTS$_1$. (**D**) Size-exclusion profiles for malE-en2NTS$_1$ in three solubilising detergents, DDM, LMPG and Brij58.

the product by centrifugation. Expression was observed for most of the N-terminal tags tested, despite an overall lower expression for the linear templates compared to an intact plasmid. Despite the low expression, two signal sequence based tags obtained from malE and ompC promoted sufficient expression, with the 26-residue malE tag producing approximately 47% more product than ompC tagged en2NTS$_1$ (Fig. 1B). Thus malE-en2NTS$_1$ cloned into pETMCSI (a kind gift from K. Ozawa and G. Otting) was therefore used for continued study.

malE-en2NTS$_1$ expression optimisation and purification. Further optimisation of malE-en2NTS$_1$ expression was carried out by testing varying Mg^{2+} concentrations, expression in the presence and absence of detergent and determining the relative yield of protein from CFPS. Titration with Mg^{2+} showed that optimal expression could be obtained at a concentration of 17 mM. Expression could be carried out in the presence of Brij35 (0.1% w/v) and Brij58 (1.5% w/v), with noticeably better expression in Brij58 because a large proportion of malE-en2NTS$_1$ was insoluble with Brij35 addition (Fig. 2A). Notably, addition of Triton X-100, dodecylphosphocholine (DPC), decyl maltoside (DM) or dodecyl maltoside (DDM), resulted in no malE-en2NTS$_1$ expression. A comparison between detergent mode-CFPS (D-CFPS) using Brij58 and P-CFPS showed P-CFPS generated higher levels of synthesised protein. Overall yields by D-CFPS and P-CFPS were 0.5–1 mg mL^{-1} and 1.5–2 mg mL^{-1} respectively. For malE-en2NTS$_1$ expressed in the P-CFPS mode, complete solubilisation of the precipitate was successfully carried out using 21 mM (1% w/v) 1-myristoyl-2-hydroxy-*sn*-glycero-3-phospho-(1′-*rac*-glycerol) (LMPG) in nickel equilibration buffer.

Purification utilised Ni-IMAC to produce a product that was $\geq$ 90% pure for both D-CFPS and P-CFPS derived malE-en2NTS$_1$ (Fig. 2B,C respectively). All samples were purified in either Brij58 (D-CFPS derived), LMPG (P-CFPS derived) or DDM (buffer exchanged from D-CFPS or P-CFPS derived malE-en2NTS$_1$). Unfortunately malE-en2NTS$_1$ was unable to be detergent exchanged into DM. Several attempts were carried out, however all attempts resulted in precipitation of malE-en2NTS$_1$. The precipitated material was determined to be

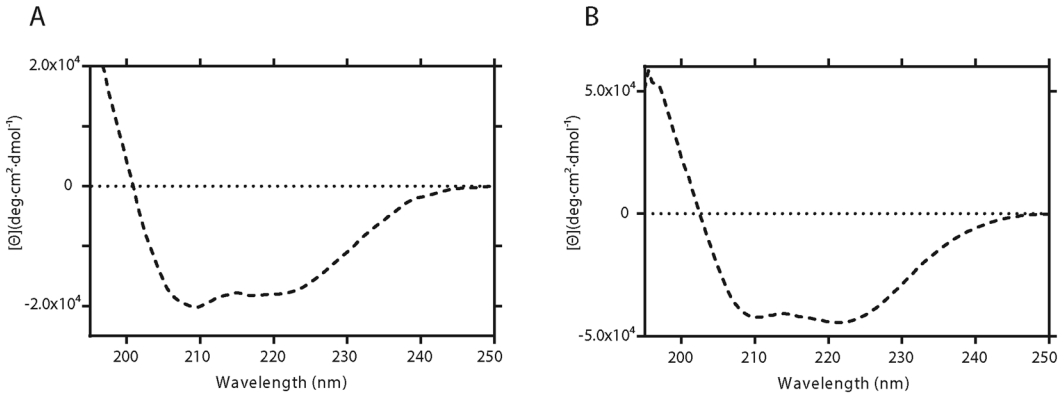

Figure 3. Circular dichroism spectra of malE-en2NTS$_1$ and *E. coli* produced en2NTS$_1$. Data are represented as mean residue ellipticity for (**A**). CFPS produced malE-en2NTS$_1$ and (**B**). *E. coli* produced en2NTS$_1$, where both show a profile exhibiting α-helical like structure, as visualised by a pronounced local minima at 208 nm and 222 nm.

Data sets	CD data/ CDpro output Algorithm: CDSSTR	CD data/ CDpro output Algorithm: CONTIN-LL	CD data/ CDpro output Algorithm: CDSSTR	CD data/ CDpro output Algorithm: CONTIN-LL	STRIDE[a] analysis of NTS$_1$-OGG7
	malE-en2NTS$_1$	malE-en2NTS$_1$	en2NTS$_1$	en2NTS$_1$	NTS$_1$-OGG7 (4BV0)
α-helix total (%)	60.5	58.6	56.1	69.3	63.1
β-strand total (%)	13	8.4	16	1	2.7
Turns (%)	13.8	23.2	13.8	4.4	7.2
Unordered (%)	10.9	9.7	14.3	25.3	6.4
Unknown (%)	—	—		—	20.6
nRMSD	0.03	0.106	0.08	0.224	—

Table 1. Percentage composition of secondary structure for malE-en2NTS$_1$ and *E. coli* produced en2NTS$_1$ compared to structural data using pdb data inputted into STRIDE. [a]STRIDE calculations were based on the NTS$_1$-OGG7 structure with the pdb accession code 4BV0. 4BV0 is a stable NTS$_1$ variant lacking most of ICL3, and most of the N- and C-terminus. In addition only 297 residues of NTS$_1$-OGG7 were identifiable compared to 374 residues of malE-en2NTS$_1$. Therefore, for this analysis, secondary structure content was calculated for 374 residues resulting in missing information for 20.6% of the protein.

malE-en2NTS$_1$ by SDS-PAGE (data not shown). For malE-en2NTS$_1$ purified in either DDM, LMPG or Brij58, size-exclusion profiles show monodisperse profiles (Fig. 2D). The varying elution volumes were predicted to be due to the different micellar properties of the solubilising detergents (Fig. S2 in Supporting Information).

Circular Dichroism and secondary structure. Circular dichroism (CD) was carried out to determine the estimated secondary structure of malE-en2NTS$_1$. The samples used for CD were derived either from D-CFPS and P-CFPS expressed malE-en2NTS$_1$. In both cases however, detergent exchange to DDM took place during the Ni-IMAC step and DDM was maintained during subsequent SEC and CD steps. The far-UV wavelength CD profile of malE-en2NTS$_1$, which includes the 26-residue malE tag, displayed a content of secondary structure consistent with that of a folded GPCR (Fig. 3A). This was broadly similar to the control CD profile obtained for *E. coli* produced en2NTS$_1$, however the mean residue ellipticity is lower for the cell-free produced material (Fig. 3B). The two double minima present at 208 and 222 nm were suggestive of a protein with a high propensity of α-helix. The reconstituted data were fitted best with the algorithms CDSSTR and CONTILL, producing the lowest nRMSD values and therefore a more accurate fit of the acquired data[19] (Table 1). When analysed, the overall secondary structure composition calculated by CDpro produced an estimation of α-helix similar to data obtained from a second program, STRIDE[20]. The calculated α-helical percentage (58–60%) and the limited amount of β-strand (8–13%) was similar to the calculated CD profile for *E. coli* produced en2NTS$_1$ as well as the amount determined for the NTS$_1$-OGG7 crystal structure (OGG7-ΔIC3, PDB: 4BV0), to which both malE-en2NTS$_1$ and en2NTS$_1$ share many of the same stabilising mutations[10] (Fig. S3 in Supporting Information). This analysis is suggestive of malE-en2NTS$_1$ assuming a structure that is consistent with correct secondary fold, however the lower value of the mean residue ellipticity is consistent with poor packing of the α-helices to form the correct tertiary structure[21]. Clearly, in the absence of the *E. coli* expressed en2NTS1 such an analysis is not possible.

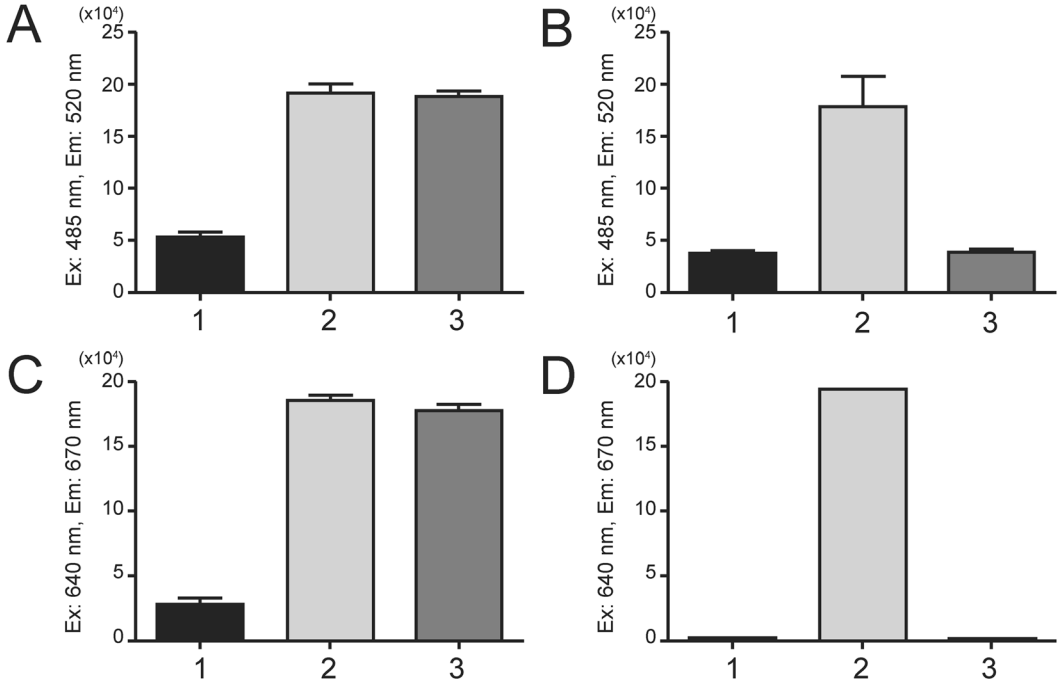

Figure 4. Streptavidin and His-tag pull down assay of CFPS malE-en2NTS$_1$ and *E. coli* expressed en2NTS$_1$. Binding assay, testing capability of binding to Biotin-NT using Streptavidin dynabeads in combination with (**A**). CFPS produced malE-en2NTS$_1$ and (**B**). The *E. coli* expressed en2NTS$_1$ control. Each graph reads 1. Receptor alone. 2. Biotin-NT plus receptor. 3. Biotin NT, receptor and unlabelled NT$_{8-13}$ competitor. Binding assay using His-tag isolation dynabeads in combination with (**C**). CFPS produced malE-en2NTS$_1$ (**D**). *E. coli* expressed en2NTS$_1$. Each graph reads 1. Receptor alone. 2. A647-NT$_{8-13}$ plus receptor. 3. A647-NT$_{8-13}$, receptor and NT$_{8-13}$ competitor. Data is presented as triplicate experiments ± SEM.

Streptavidin and His$_6$-tag pulldown assays of malE-en2NTS$_1$. Automated streptavidin binding experiments were carried out using the kingfisher particle processor. Streptavidin-coated dynabeads were used to capture biotinylated NT, which was subsequently used to capture CFPS produced malE-en2NTS$_1$ (Fig. 4A). *E. coli* expressed en2NTS$_1$ (Fig. S3) served as a control for expected interaction of the receptors with the NT$_{8-13}$ ligand (Fig. 4B). The experimental set up included three conditions; 1: Receptor alone, 2: biotinylated-NT and receptor and 3: biotinylated-NT, receptor and unlabelled NT$_{8-13}$ competitor. No binding of malE-en2NTS$_1$ or of en2NTS$_1$ was detected to the streptavidin dynabeads in the absence of bound biotin-NT. Addition of biotin-NT promoted binding of malE-en2NTS$_1$ and en2NTS$_1$ to the beads. Addition of competing unlabelled NT$_{8-13}$ caused a reduced level of bound en2NTS$_1$, but did not change the level of bound malE-en2NTS$_1$ to the biotin-NT-coated streptavidin dynabeads. For malE-en2NTS$_1$, samples obtained following Ni-IMAC in the detergents Brij58, LMPG or DDM produced the same result, as did samples purified by SEC in DDM (data not shown).

In light of the streptavidin pulldown experiments, an alternative approach was attempted. malE-en2NTS$_1$ was designed with a His$_{10}$-tag at its C-terminus, a trait that is exploited during its purification. With this in mind, the His-tag was used to reverse the original streptavidin method for detection of possible binding of NT$_{8-13}$. By coupling the malE-en2NTS$_1$ receptor to His-tag isolation dynabeads, detection of binding can be made through Alexa647 fluorescently labelled NT[14]. Once again, malE-en2NTS$_1$ binding experiments could be compared in a similar manner to the *E. coli* expressed en2NTS$_1$ control which can also be captured via its His-tag. Results from several experiments however produced similar results to the previous streptavidin assay (Fig. 4C,D). In the absence of bound receptor, A647-NT$_{8-13}$ showed no interaction with the His-tag isolation dynabeads. Binding of both receptors to the His-tag isolation dynabeads, promoted binding of A647-NT$_{8-13}$. The co-incubation of excess unlabelled NT$_{8-13}$ as a competitor resulted in no dissociation of A647-NT$_{8-13}$ from CFPS produced malE-en2NTS$_1$, whereas complete competition of A647-NT$_{8-13}$ binding was observed from *E. coli* produced en2NTS$_1$ immobilised beads (Fig. 4D).

^{1}H-^{13}C SOFAST HMQC NMR of en2NTS$_1$. $^{13}CH_3$- methionine labelled malE-en2NTS$_1$ was purified from either P-CFPS or D-CFPS derived sources in DDM and Brij58 detergents respectively. malE-en2NTS$_1$ in the NT agonist bound state was recorded by adding excess NT$_{8-13}$ in a ratio of 10:2 NT$_{8-13}$:receptor (100 µM:20 µM). Following NMR acquisition, the sample was checked for any precipitation by visual inspection of the sample. Spectra were obtained for malE-en2NTS$_1$ (apo and 100 µM NT$_{8-13}$) in the presence of 1 mM DDM or 1 mM Brij58.

MalE-en2NTS1 has three methionines in the malE tag and nine within the transmembrane domain (Figs S3 and S4 in Supporting Information). However, the spectra for apo malE-en2NTS$_1$ in both detergents displayed two broad signals (Fig. 5A,C) compared to *E. coli* derived en2NTS$_1$ in DDM, which showed clearly defined resonances

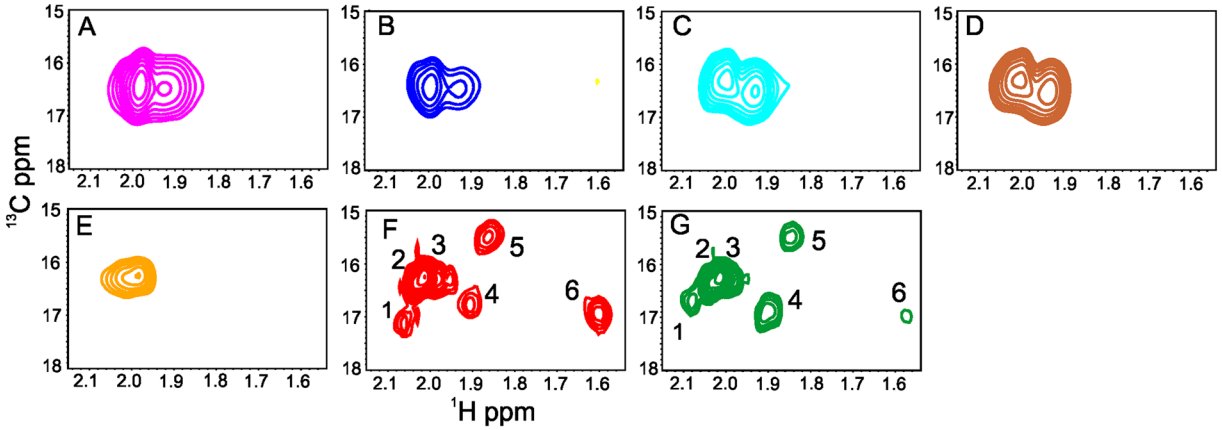

Figure 5. ^{1}H-^{13}C SOFAST-HMQC spectra of $^{13}CH_3$-methionine labelled malE-en2NTS$_1$ and en2NTS$_1$. (**A**). malE-en2NTS$_1$ (apo) in DDM (**B**). malE-en2NTS$_1$ (100 μM NT_{8-13}) in DDM. (**C**) malE-en2NTS$_1$ (apo) in Brij58. (**D**) malE-en2NTS$_1$ (100 μM NT_{8-13}) in Brij58. (**E**) malE-en2NTS$_1$ (50 μM NT_{8-13}) in POPC nanodiscs. (**F**) en2NTS$_1$ in DDM. (**G**) en2NTS$_1$ (500 μM NT_{8-13}) in DDM.

for at least six of nine possible methionine signals (Fig. 5F). Alternatively, addition of NT_{8-13} to CFPS-derived malE-en2NTS$_1$ promoted no change in the size of the resonance, nor was there any noticeable change in chemical shift (Fig. 5B,D) whereas addition of NT_{8-13} to *E. coli* derived en2NTS$_1$ resulted in chemical shift and/or line width changes for four of the resonances (Fig. 5G). Of particular note was the observed shape of both P-CFPS and D-CFPS derived forms of malE-en2NTS$_1$, where a comparison of resonances derived from samples purified from D-CFPS and P-CFPS malE-en2NTS$_1$ (Fig. 5A,C) indicate, that regardless of the CFPS method for malE-en2NTS$_1$ production, the final purified forms are displaying similar properties.

MalE-en2NTS$_1$ labelled with $^{13}CH_3$- methionine was expressed in the presence of POPC nanodiscs. NMR was carried out on Ni-IMAC purified malE-en2NTS$_1$, in the same manner used for detergent purified malE-en2NTS$_1$. From the spectra, only a large single resonance was detectable, although the line-width of this single resonance compared to DDM/Brij58 solubilised malE-en2NTS$_1$ appeared narrower (Fig. 5E). Comparison to the spectra obtained for en2NTS$_1$ (Fig. 5F) show none of the defined resonances expected of a protein adopting a distinct tertiary structure.

Following NMR acquisition, the sample was applied to SEC to identify whether the nanodisc fraction still maintained the expected elution profile. Nanodiscs that utilise the MSP1D1 scaffold have a defined diameter of ~100 Å or 10 nm without embedded membrane protein and may be slightly larger with protein embedded[22,23]. When compared to protein standards, nanodiscs of correct size eluted at the same volume as catalase, due to their shared Stokes diameter. For the malE-en2NTS$_1$/POPC complex, the elution did not overlap with the expected elution for catalase, instead eluting in the predetermined void-volume, which is indicative of misfolded protein (Fig. S5 in Supporting Information). From the SDS-PAGE of the fractions obtained by SEC, it can be concluded that the protein was associated with the MSP1D1 scaffold, however the "complexes" were very large, suggesting that malE-en2NTS$_1$ had possibly promoted disruption of the disc structure.

It should be noted here, that we have made attempts to incorporate purified malE-en2NTS$_1$ into nanodiscs and liposomes composed of POPC, DMPC or *E. coli* total lipid extract. Regrettably all attempts to reconstitute malE-en2NTs$_1$ resulted in protein destabilisation and protein precipitation following detergent removal by use of biobeads or dialysis. For nanodisc reconstitution, changing the incubation time, ratios of malE-en2NTS1, lipid and MSP1D1 scaffold protein did not prevent protein precipitation.

Discussion

G-protein coupled receptors are a diverse set of membrane proteins that respond to an equally diverse range of external stimuli. The many roles that GPCRs play in human physiology highlights their importance and therefore their continued study. Over the years, techniques to produce GPCRs recombinantly have led to an expansion in the details surrounding their structure and function. GPCRs have typically been generated via insect (*S. frugiperda or T. ni)* or yeast (*P. pastoris)* cell expression, which allows for processing by the secretory pathway[24,25]. Alternate expression methodologies include that of *E. coli* expression, by both membrane integration[10,26,27] or by inclusion body formation[8]. Cell-free protein synthesis offers a fourth alternative for the production of GPCRs[11–13], with exciting prospects for introducing unnatural amino acids and for allowing direct access to solubilising detergent, all of which formed the basis for this work.

Outlined here is the design, production, purification and initial characterisation of cell-free produced malE-en2NTS$_1$, a thermostable NTS$_1$ receptor[14]. This receptor was chosen for its proven ability for expression in *E. coli* cell systems (the basis for the CFPS extract used here), high stability in short chained detergents and at elevated temperature and more recently a similar variant was successfully crystallised and its structure determined[10].

Work proceeded first with en2NTS$_1$ by designing suitable N-terminal tags for the quick generation of PCR templates. This methodology allows for the production of multiple templates for rapid determination of expression[16–18,28,29]. Nine tags were chosen with PCR templates for all tags generated in one day. CFPS proceeded the following day and determination of protein expression on the third day. Ultimately CFPS of the malE-tagged

en2NTS$_1$ demonstrated that it was the optimal construct, with high levels of protein production in the 1.5–2 mg/mL range.

Introduction of individual detergents into the CFPS reactions was shown to promote or perturb malE-en2NTS$_1$ solubility. Of the detergents tested, only Brij35 and Brij58 resulted in soluble protein expression, with Brij58 promoting complete solubilisation (Fig. 2A). Alternatively samples of malE-en2NTS$_1$ derived from CFPS reactions in the P-CFPS mode were able to be solubilised into a refolding solution containing 1% (w/v) LMPG. The properties of malE-en2NTS$_1$ detergent solubilisation, during D-CFPS and following P-CFPS, show consistencies with previously published work[30]. Surprisingly however, problems arose during detergent exchange steps, where either Brij58 or LMPG were exchanged to DM. In all instances of detergent exchange to DM, protein destabilisation was observed, culminating in overt protein precipitation. Comparatively, detergent exchange into DDM resulted in no precipitation. malE-en2NTS$_1$ destabilisation in DM was not expected, considering the reported stability of en2NTS$_1$ in shorter and thus more destabilising detergents, such as octyl-glucoside (OG)[10,14]. However, the observed differences in stability were noted to possibly be in part due to the slight differences in protein sequence between malE-en2NTS$_1$ and en2NTS$_1$, such as the addition of the malE-tag.

Investigation of secondary structure by CD showed that malE-en2NTS$_1$ possessed the expected α-helical elements of a folded GPCR and matched the estimated secondary structure elements of the *E. coli* produced en2NTS1 and the solved NTS1-OGG7 structure. However, despite the optimistic structural characteristics of malE-en2NTS$_1$, the protein bound NT$_{8-13}$ non-specifically using either NT immobilised streptavidin beads or receptor immobilised His-tag isolation dynabeads. The ligand binding experiments of malE-en2NTS$_1$ could once again be compared with active/folded en2NTS$_1$ isolated from *E. coli*. These data indicate that despite having consistent secondary structure elements, it possibly had not adopted a suitably discrete tertiary structure, which prevented the correct ligand association and subsequent competition. ^{1}H-^{13}C HMQC SOFAST NMR experiments showed quite conclusively that malE-en2NTS$_1$ does not exhibit the same proper tertiary structure and therefore was not behaving in accordance with a correctly folded receptor. Comparisons to the *E. coli* produced en2NTS$_1$, which does bind peptide as expected and exhibited defined tertiary structure by NMR, is further evidence for the lack of defined tertiary structure for CFPS synthesised malE-en2NTS$_1$.

The noted stability of NTS$_1$ engineered variants expressed in *E. coli*[14], in comparison to CFPS produced malE-en2NTS$_1$, may indicate that a number of structural features need to be attained prior to their purification; structural features that are not easily attainable in a CF system, in the absence of a lipid bilayer and membrane insertion machinery. When expressed in *E. coli*, en2NTS$_1$ is shuffled into the lipid bilayer directed by the N-terminally fused MBP. Once exposed to the membrane folding pathway at the SecYEG-translocon (SecYEG), several factors ensure that packing of the α-helical TM segments occurs correctly and that interhelical contacts are established[31]. Without the assistance of the SecYEG and associated protein chaperones, membrane proteins are thought to rapidly collapse into non-native conformers[32]. If this is the case, then refolding of malE-en2NTS$_1$ by employing a mild LMPG solubilisation or directly into a detergent may not be sufficient to reverse any structure assumed during *in vitro* translation.

It is also possible that thermal stability of en2NTS$_1$ gained through successive rounds of directed evolution does not increase the propensity to adopt the correct fold, unassisted, from an unfolded/semi-folded state. Likewise, malE-en2NTS$_1$ derived from CFPS did not respond in a manner expected of a functional receptor. While most native GPCRs would unfold in conditions where short chain detergents are present, en2NTS$_1$ produced in *E. coli* does not. Thus, the structural stability of bacterially produced en2NTS$_1$ in detergents such as DDM, DM or OG is contingent on the receptor first being properly folded in the *E. coli* membrane environment conducible to receptor folding, prior to detergent solubilisation.

One approach to supplying nascent malE-en2NTS$_1$ with a lipid bilayer was undertaken by supplementing the CFPS reaction with preformed nanodiscs[33] comprised of a POPC core and MSP1D1 scaffolding. Recently there have been several reports of direct CF expression of GPCRs into lipid nanodiscs[34,35]. These embedded receptors were also reported to exhibit activity, therefore offering a new method for obtaining this class of receptor in a biologically active form. Successful CFPS expression of malE-en2NTS$_1$ in the presence of nanodiscs and their subsequent purification also hinted at the possibility of this receptor being embedded within the nanodisc lipid core. As before, the ^{1}H-^{13}C HMQC SOFAST acquisition was unable to detect individual dispersed resonances exhibited by *E. coli* produced en2NTS$_1$. Unfortunately, a comparison of malE-en2NTS$_1$ associated with the POPC nanodiscs showed a single resonance dispersal pattern similar to that of detergent solubilised malE-en2NTS$_1$. Following NMR acquisition, the malE-en2NTS$_1$/nanodisc sample was applied to gel filtration, which confirmed the aberrant NMR results were most likely due to misfold and collapse of the preformed nanodisc structure.

While the goals we set out to achieve were not met, a number of useful procedures could be implemented as generic means for assessing membrane proteins produced by CFPS. Notably the use of competition binding assays to identify whether interactions with target substrates/ligands are correct. Alternatively, if a suitable ligand is unavailable, isotopic labelling during CFPS, such as $^{13}CH_3$-methionine, can be used for an economic and rapid determination of protein fold.

For malE-en2NTS$_1$, it seems likely that it would not be possible to obtain a functional form of this receptor when derived from CFPS, unless a more radical approach to its production is undertaken. This would require malE-en2NTS$_1$ expression to be undertaken in the presence of a fully functional membrane translocon. This has been trialled before with microsomes or through trials of membrane incorporation with components of SecYEG and affiliated proteins[36]. In another test case, GPCRs have been incorporated into giant unilamellar vesicles originating from endoplasmic reticulum[37]. Alternatively, incorporation of *E. coli* microsomes derived from inner membrane vesicles (IMV) could possibly serve as a substitute to ER derived membranes. One study has shown *E. coli* IMVs are capable of incorporating two *E. coli* transporters, mannitol permease (MtlA) and the tetracycline pump (TetA)[38]. Of the total protein expressed, MtlA and TetA were successfully incorporated into the microsome bilayer at 38% (130 µg/mL) and 66% (570 µg/mL) respectively[38]. The yields for CFPS membrane incorporation are

currently medium-low for these types of systems, owing to limitations in incorporation rates and total membrane area. Whether non-*E. coli* derived proteins could be incorporated into an *E. coli* based CFPS system with *E. coli* derived IMVs, is a matter for future investigation. However this may offer a potential method for production of folded and functional *in vitro* synthesised membrane protein and GPCRs as a whole.

Methods

enNTS1 plasmid construction. PCR was used to generate several different linear fused-gene DNA templates of enNTS1, each with their own unique expression tag for quick determination of levels of expression by CFPS (Fig. S1 in Supporting Information). The constructs were designed to have en2NTS$_1$ preceded by an N-terminal expression tag followed by a 3C-protease site and succeeded by a C-terminal His$_{10}$-tag. The following expression tags were selected based on previously reported accounts: the signal sequences of *E. coli* ompA, ompC, malE[16], an HA-tag (Roche pIVEX2.6d vector), truncated T7-tag (MASMTG)[18], and the systematically designed expression tags AT, SER, H and G[17]. Once determination of optimal en2NTS$_1$ expression was made, the thermostabilised en2NTS$_1$ gene was subcloned using the NdeI and EcoRI restriction sites into pETMCSI. Generation of the malE-en2NTS$_1$ fusion, was generated by a combination of overlap PCR, using the primers P1, P8, P9, P14 and P15 (Table S1 in Supporting Information).

Continuous exchange cell-free protein synthesis. Preparation of *E. coli* BL21(DE3) S30 extracts as well as the CFPS reaction was performed as described by Apponyi *et al.*[39] with minor changes described below. *E. coli* S30 extract production was prepared using the BL21(DE3) Rosetta strain. These latter cells were grown using the YTPG growth medium described in Choi *et al.*[40]. The cell culture OD_{600} was monitored during the growth phase. Once the OD_{600} reached 0.85, the culture was induced with 1 mM IPTG allowing production of T7RNAP to take place, thus preventing separate expression and purification of this vital component.

Each CFPS reaction was composed of 0.8 mM rNTPs (CTP, UTP, GTP), 1.2 mM ATP, 55 mM HEPES pH 7.2, 68 µM Folinic acid, 0.64 mM 3′,5′-cyclic AMP, 1 mM DTT, 27.5 mM Ammonium acetate, 1 mM amino acids, 80 mM creatine phosphate, 290 mM Potassium acetate, 16–17 mM Magnesium acetate, 7.7 mM Sodium azide, 1x protease inhibitor, 1 mM six amino acid mix (RCWMDE)[30,41], 0.3 U RNase inhibitor, 250 µg mL^{-1} creatine kinase, 175 µg mL^{-1} *E. coli* total tRNA, 20–40% (v/v) S30 extract, 16 µg mL^{-1} DNA plasmid template. For reactions requiring use of $^{13}CH_3$-methionine, amino acid stocks incorporated 0.5 mM $^{13}CH_3$-methionine and 1 mM of the 19 other amino acids.

For continuous exchange CFPS the reaction chamber was prepared as described in Apponyi *et al.*[39]. The reaction chamber was separated from a feeder chamber which supplies new substrate for continued protein production. This was achieved by enclosing the contents of the reaction chamber (S30 extract, plasmid DNA, RNase inhibitor, creatine kinase and *E. coli* tRNA) in dialysis tubing. The dialysis bag is then placed in a feeder solution which supplies new substrate and also serves to minimise undesirable by-products from the protein synthesis reaction. Reactions were expressed in a 1:14 volume ratio (reaction chamber: feeder chamber volume) and incubated at 30 °C with orbital shaking at 160 rpm for 16 hours. Protein expression was carried out in either the presence or absence of detergent or nanodiscs; D-CFPS, P-CFPS or nanodisc (ND-CFPS) modes respectively.

Nanodisc production. Nanodisc production and assembly was performed with the MSP1D1 construct according to previously established protocols[42]. For this work, POPC nanodiscs with a diameter of ~100 Å were produced and utilised during CFPS at a concentration of 50 µM.

Protein purification of protein from cell-free synthesis. *Precipitate mode CFPS – protein solubilisation.* Precipitated malE-en2NTS$_1$ produced by P-CFPS was first separated from the overnight reaction mix by centrifugation at 17,000 × g for 10 minutes. The isolated malE-en2NTS$_1$ required an initial detergent solubilisation step in 21 mM LMPG in nickel equilibration buffer (20 mM Na_2HPO_4-NaH_2PO_4 pH 7.5, 500 mM NaCl, 5 mM imidazole pH 7.5). The CFPS produced malE-en2NTS$_1$ was allowed to mix for one hour with shaking at room temperature. Once solubilisation was complete, the solution was clarified by centrifugation at 17,000 × g for 10 minutes. The clarified solution was then used for Ni-immobilised metal affinity chromatography (Ni-IMAC).

Detergent mode CFPS. Following overnight D-CFPS of malE-en2NTS$_1$, the final reaction required solution clarification by centrifugation at 17,000 × g for 10 minutes. The sample solution was then adjusted to match the nickel equilibration buffer by dilution whilst maintaining the minimum CMC of the utilised detergent. This final solution was then used for Ni-IMAC.

Chromatography purification. malE-en2NTS$_1$ samples were incubated with 2 mL of prequilibrated Ni-sepharose (GE Healthcare) for 1 hour at 4 °C. After collecting the flow through, the Ni-sepharose was washed with 10 column volumes of buffer (20 mM Na_2HPO_4-NaH_2PO_4 pH 7.5, 500 mM NaCl, 5 mM imidazole pH 7.5, and appropriate detergent). If detergent exchange into DDM (20 mM or 1% (w/v)) was to be incorporated, this would occur during the wash step. Protein was eluted using 5 column volumes of elution buffer (20 mM Na_2HPO_4-NaH_2PO_4 pH 7.5, 500 mM NaCl, 500 mM imidazole pH 7.5, and appropriate detergent). Detergent concentrations were dependent on the individual CMC of the detergent used.

Ni-IMAC purified malE-en2NTS$_1$ was loaded onto a Superdex200 10/300 GL column pre-equilibrated with 20 mM Na_2HPO_4-NaH_2PO_4 pH 7.5, 150 mM NaCl, and appropriate detergent. The size exclusion step was carried out using an FPLC system (Äkta basic, GE healthcare) with buffer kept at 4 °C at a rate of 0.4 mL/min and detected by absorbance at 280 nm. Fractions of importance were collected and analysed by SDS-PAGE for purity.

en2NTS$_1$ expression and purification from *Escherichia coli*. *Cloning and expression.* The en2NTS$_1$ sequence was subcloned into a pQE-30-derived vector. The open reading frame of the modified vector encoded

an N-terminal maltose-binding protein signal sequence (MBPss), followed by a His_{10}-tag, a maltose binding protein (MBP), a NNNNNNNNNG linker and a HRV 3 C protease site which were linked via a BamHI restriction site (resulting in additional residues GS) to residue T42 of the receptor. C-terminally T420 of the receptor was linked via a NheI restriction site (resulting in additional residues AS) to an Avi-tag for *in vivo* biotinylation, a HRV 3 C protease site, a GGSGGS linker and a monomeric ultra-stable green fluorescent protein (musGFP)[43], which is followed by a second His_{10}-tag.

Expression and $^{13}CH_3$-methionine labelling of the MBP-en2NTS_1-musGFP fusion protein was carried out in *E. coli* C43(DE3) (Lucigen) following an adapted protocol described by Van Duyne *et al.*[44].

Chromatography purification. Cell pellets were resuspended in 100 mM HEPES, 400 mM NaCl, 20% Glycerol, pH 8 with 1x EDTA free protease inhibitor tablet (Roche), 100 mg Lysozyme, 10 mg DNAse and sonicated on ice. Following sonication 15 mL of DM solution (1.6 g n-decyl-β-D-maltopyranoside, Anagrade (Antrace) dissolved overnight in water) and 15 mL of CHS/CHAPS solution (0.12 g cholesterol hemi succinate (Sigma) and 0.6 g CHAPS-hydrate (Sigma) dissolved overnight in water) were added and the volume was adjusted to 100 mL. The solubilisation mix was left gently rocking for 2 h at 4 °C. Cell debris was removed by centrifugation.

Filtered (45 µm) supernatant was adjusted to 10 mM imidazole, passed over 6 mL of Talon resin, washed with 2 × 25 mL of 25 mM HEPES, 500 mM NaCl, 10% Glycerol, 0.15% DM, 10 mM Imidazole, 0.2 mM PMSF, 8 mM ATP, 10 mM MgCl2, pH 8. Detergent was exchanged to DDM (n-decyl-β-D-maltopyranoside) (Anagrade, Anatrace) by washing with 2 × 25 mL of 25 mM HEPES, 100 mM NaCl, 10% Glycerol, 0.05% DDM, 0.2 mM PMSF, pH 8. The fusion protein was eluted using 15 × 1 mL of 25 mM HEPES, 100 mM NaCl, 10% Glycerol, 0.05% DDM, 350 mM Imidazole, 0.2 mM PMSF, pH 8.

The eluate was concentrated to 1 mL using an Amicon Ultra 15 concentrator with 100 kDa cutoff (Millipore); buffer exchanged using a PD10 desalting column (GE Healthcare) into 25 mM HEPES, 300 mM NaCl, 10% Glycerol, 0.05% DDM, pH 8. Proteolytic cleavage was carried out by adding 100 mM of Na_2SO_4, 1 mM TCEP and 30 µL of GST-tagged HRV 3 C protease (96 µM stock produced in house) to the 4 mL PD10 eluate and rocking gently for 16 h at 4 °C. The protease was removed by mixing for 1 h at 4 °C with 2 mL of Glutathione Sepharose 4B (GE Healthcare). The flow-through was collected and the GST resin washed with 15 mL of buffer. GST flow-through and wash were combined, adjusted to 5 mM Imidazole and transferred to a gravity flow column containing 6 mL of Talon resin equilibrated with 2 × 25 mL of 25 mM HEPES, 300 mM NaCl, 10% Glycerol, 0.05% DDM, pH 8. The mixture was rocked for 45 min at 4 °C. The flow-through containing cleaved enNTS1 was collected, the beads washed with 3 × 10 mL of buffer.

The flow-through and washes were combined and concentrated to 450 µL using an Amicon Ultra 15 concentrator with 30 kDa cutoff (Millipore). The concentrate was transferred to an Eppendorf tube and centrifuged in a table-top centrifuge (10000 rpm, 4 °C, 10 min) to separate any aggregated protein. The supernatant was loaded and further purified on a Superdex 200 10/300 Increase column (GE Healthcare) equilibrated with 50 mM potassium phosphate, 100 mM NaCl, 0.02% DDM, pH 7.4.

Circular dichroism spectroscopy. Far UV circular dichroism (CD) spectroscopy was carried out to estimate the secondary structure of malE-en2NTS_1. Measurements were performed on an AVIV Model 410 SF spectropolarimeter (Aviv) equipped with a temperature controlled jacket set at 25 °C. malE-en2NTS_1 samples were maintained in a minimal salt buffer (20 mM Na_2HPO_4-NaH_2PO_4 pH 7.5, 50 mM NaCl, 0.3 mM DDM). Wavelength scans were assayed at the far-UV range from 250 to 190 nm at 0.5 nm intervals and in triplicate for averaging. Protein samples (0.1 mg mL^{-1}) were housed in a 1-mm light path quartz cuvette (Starna). Data measured from wavelengths 250–190 nm were expressed as mean residue ellipticity [θ] and fitted using the CDpro software[45] running three algorithms to provide an estimate of the secondary structure composition; SELCON3[46], CDSSTR[47] and CONTINLL[48]. All algorithms used the protein reference set SMP56[49] which includes 43 soluble proteins and 13 membrane proteins for comparison.

Ligand binding assay. Ligand binding assays of malE-en2NTS_1 and en2NTS_1 were performed on the KingFisher Flex Magnetic Particle Processor (Thermo Scientific) carried out at 4 °C. For malE-en2NTS_1 pulldown experiments, two different dynabead matrices were used; Streptavidin coupled M-280 dynabeads or His-tag isolation and pulldown dynabeads (Life Technologies). Streptavidin coupled M-280 dynabeads were incubated with biotinylated neurotensin (produced in house via reaction between maleimide-PEG2-Biotin and a cysteine modified NT) for one hour. malE-en2NTS_1 receptor binding was assessed by binding of a primary mouse Anti-His antibody (1:1000, Cell Signalling Technologies) followed by binding of anti-mouse-Alexa488 antibody (1:5000, Life Technologies). Competition was assessed through incubation of unlabelled $NT_{8-13.}$ The mixing protocol was as follows, with washing for 10 minutes between each step: streptavidin dynabeads were incubated with biotinylated NT for one hour, then with malE-en2NTS_1 or en2NTS_1 ± competitor NT_{8-13} for another hour, with mouse Anti-His antibody (1:1000) for one hour, and a final incubation with secondary Anti-mouse-Alexa488 (1:5000) for one hour, before dynabead release. Dynabeads transferred to a 96-well non-binding Greiner black plate were assessed for fluorescence of Alexa488 (495 nm excitation and emission at 519 nm) measured on a POLARstar OMEGA plate reader (BMG Labtech). Alternatively His-tag isolation and pulldown dynabeads were used to capture malE-en2NTS_1 or en2NTS_1 for one hour. Ligand binding was assessed through binding of the Alexa647 labelled NT_{8-13}[50] and competition assessed by introducing unlabelled NT_{8-13}. Alexa647 fluorescence (650 nm excitation and emission at 668 nm) were also measured on a POLARstar OMEGA plate reader.

NMR Spectroscopy. Purified $^{13}CH_3$-Methionine labelled malE-en2NTS_1 or en2NTS_1 was exchanged in NMR buffer (20 mM Na_2HPO_4-NaH_2PO_4 pH 7.5, 50 mM NaCl, 10% D_2O) and placed into 5 mm NMR sample tubes. The NMR buffer included detergent when required (1 mM DDM, 1 mM LMPG). NMR spectra malE-en2NTS_1

were acquired on approximately 20 μM malE-en2NTS$_1$ ± 100 μM NT$_{8-13}$, or 30 μM en2NTS$_1$ ± 50 μM NT$_{8-13}$ with a Bruker Avance 800 MHz spectrometer equipped with a cryogenic probe. 2D ^{1}H-^{13}C SOFAST-HMQC spectra[51] were typically recorded at 298 K with spectral widths of 9,615 Hz (1,024 data points) and 8,000 Hz (128 data points) for the ^{1}H and ^{13}C dimensions respectively with a relaxation delay of 400 ms. The ^{13}C carrier frequency was positioned at 17 ppm, and the ^{1}H at 4.7 ppm, while band selective ^{1}H pulses were centred at 2 ppm. Prior to Fourier transformation, data were multiplied by cosine-bells and zero-filled once in each dimension. All NMR data was processed in NMRPipe[52] and plotted in Sparky (Goddard, T.D. and Kneller, D.G., University of California, San Francisco).

References

1. Fredriksson, R., Lagerström, M. C., Lundin, L.-G. & Schiöth, H. B. The G-Protein-Coupled Receptors in the Human Genome Form Five Main Families. Phylogenetic Analysis, Paralogon Groups, and Fingerprints. *Mol. Pharmacol* **63**, 1256–1272 (2003).
2. Foord, S. M. *et al*. International Union of Pharmacology. XLVI. G Protein-Coupled Receptor List. *Pharmacol. Rev.* **57**, 279–288 (2005).
3. Rosenbaum, D. M., Rasmussen, S. G. F. & Kobilka, B. K. The structure and Function of G-Protein-Coupled Receptors. *Nature* **459**, 356–363 (2009).
4. Schöneberg, T. *et al*. Mutant G-protein-coupled receptors as a cause of human diseases. *Pharmacol. Ther.* **104**, 173–206 (2004).
5. Stevens, R. C. *et al*. The GPCR Network: A Large-Scale Collaboration to Determine Human GPCR Structure and Function. *Nat. Rev. Drug Discov.* **12**, 25–34 (2013).
6. Magnani, F., Shibata, Y., Serrano-Vega, M. J. & Tate, C. G. Co-evolving stability and conformational homogeneity of the human adenosine A2a receptor. *Proc. Natl. Acad. Sci. USA* **105**, 10744–10749 (2008).
7. Serrano-Vega, M. J., Magnani, F., Shibata, Y. & Tate, C. G. Conformational thermostabilization of the β1-adrenergic receptor in a detergent-resistant form. *Proc. Natl. Acad. Sci* **105**, 877–882 (2008).
8. Park, S. H. *et al*. Structure of the chemokine receptor CXCR1 in phospholipid bilayers. *Nature* **491**, 779–783 (2012).
9. Shibata, Y. *et al*. Thermostabilization of the neurotensin receptor NTS1. *J. Mol. Biol.* **390**, 262–277 (2009).
10. Egloff, P. *et al*. Structure of signaling-competent neurotensin receptor 1 obtained by directed evolution in *Escherichia coli*. *Proc. Natl. Acad. Sci* **111**, E655–E662 (2014).
11. Ishihara, G. *et al*. Expression of G protein coupled receptors in a cell-free translational system using detergents and thioredoxin-fusion vectors. *Protein Expr. Purif.* **41**, 27–37 (2005).
12. Sansuk, K. *et al*. GPCR proteomics: mass spectrometric and functional analysis of histamine H1 receptor after baculovirus-driven and *in vitro* cell free expression. *J. Proteome Res.* **7**, 621–629 (2008).
13. Basu, D., Castellano, J. M., Thomas, N. & Mishra, R. K. Cell-free protein synthesis and purification of human dopamine D2 receptor long isoform. *Biotechnol. Prog.* **29**, 601–608 (2013).
14. Scott, D. J. & Plückthun, A. Direct Molecular Evolution of Detergent-Stable G-Protein-Coupled Receptors Using Polymer Encapsulated Cells. *J. Mol. Biol.* **425**, 662–677 (2012).
15. Bentele, K., Saffert, P., Rauscher, R., Ignatova, Z. & Blüthgen, N. Efficient translation initiation dictates codon usage at gene start. *Mol. Syst. Biol.* **9**, 675 (2013).
16. Ahn, J.-H., Hwang, M.-Y., Lee, K.-H., Choi, C.-Y. & Kim, D.-M. Use of signal sequences as an *in situ* removable sequence element to stimulate protein synthesis in cell-free extracts. *Nucleic Acids Res* **35**(e21), 1–8 (2007).
17. Haberstock, S. *et al*. A systematic approach to increase the efficiency of membrane protein production in cell-free expression systems. *Protein Expr. Purif.* **82**, 308–316 (2012).
18. Wu, P. S. C. *et al*. Cell-free transcription/translation from PCR-amplified DNA for high-throughput NMR studies. *Angew. Chem. Int. Ed Engl.* **46**, 3356–3358 (2007).
19. Kelly, S. M., Jess, T. J. & Price, N. C. How to study proteins by circular dichroism. *Biochim. Biophys. Acta* **1751**, 119–139 (2005).
20. Heinig, M. & Frishman, D. STRIDE: a web server for secondary structure assignment from known atomic coordinates of proteins. *Nucleic Acids Res* **32**, W500–502 (2004).
21. Martin, S. R. & Schilstra, M. J. Circular dichroism and its application to the study of biomolecules. *Methods Cell Biol* **84**, 263–293 (2008).
22. Boldog, T., Grimme, S., Li, M., Sligar, S. G. & Hazelbauer, G. L. Nanodiscs separate chemoreceptor oligomeric states and reveal their signaling properties. *Proc. Natl. Acad. Sci* **103**, 11509–11514 (2006).
23. Bayburt, T., Leitz, A., Xie, G., Oprian, D. & Sligar, S. Transducin activation by nanoscale lipid bilayers containing one and two rhodopsins. *J. Biol. Chem.* **282**, 14875–14881 (2007).
24. Massotte, D. G protein-coupled receptor overexpression with the baculovirus-insect cell system: a tool for structural and functional studies. *Biochim. Biophys. Acta* **1610**, 77–89 (2003).
25. Macauley-Patrick, S., Fazenda, M. L., McNeil, B. & Harvey, L. M. Heterologous protein production using the Pichia pastoris expression system. *Yeast Chichester Engl* **22**, 249–270 (2005).
26. Tucker, J. & Grisshammer, R. Purification of a rat neurotensin receptor expressed in *Escherichia coli*. *Biochem. J.* **317**(Pt 3), 891–899 (1996).
27. Weiß, H. M. & Grisshammer, R. Purification and characterization of the human adenosine A(2a) receptor functionally expressed in *Escherichia coli*. *Eur. J. Biochem. FEBS* **269**, 82–92 (2002).
28. Ahn, J.-H., Keum, J.-W. & Kim, D.-M. Expression Screening of Fusion Partners from an *E. coli* Genome for Soluble Expression of Recombinant Proteins in a Cell-Free Protein Synthesis System. *PloS One* **6**, e26875 (2011).
29. Kralicek, A. V. *et al*. A PCR-directed cell-free approach to optimize protein expression using diverse fusion tags. *Protein Expr. Purif.* **80**, 117–124 (2011).
30. Schwarz, D. *et al*. Preparative scale expression of membrane proteins in *Escherichia coli*-based continuous exchange cell-free systems. *Nat. Protoc.* **2**, 2945–2957 (2007).
31. Bowie, J. U. Solving the membrane protein folding problem. *Nature* **438**, 581–589 (2005).
32. Hartl, F. U. & Hayer-Hartl, M. Converging concepts of protein folding *in vitro* and *in vivo*. *Nat. Struct. Mol. Biol.* **16**, 574–581 (2009).
33. Bayburt, T. H., Yelena, V. G. & Sligar, S. G. Directed self-assembly of monodisperse phospholipid bilayer Nanodiscs with controlled size. *Nano Lett.* **2**, 853–856 (2002).
34. Gao, T. *et al*. Characterization of De Novo Synthesized GPCRs Supported in Nanolipoprotein Discs. *PLoS ONE* **7**, e44911 (2012).
35. Yang, J.-P., Cirico, T., Katzen, F., Peterson, T. C. & Kudlicki, W. Cell-free synthesis of a functional G protein-coupled receptor complexed with nanometer scale bilayer discs. *BMC Biotechnol.* **11**, 57 (2011).
36. Hovijitra, N. T., Wuu, J. J., Peaker, B. & Swartz, J. R. Cell-free synthesis of functional aquaporin Z in synthetic liposomes. *Biotechnol. Bioeng.* **104**, 40–49 (2009).
37. Fenz, S. F., Sachse, R., Schmidt, T. & Kubick, S. Cell-free synthesis of membrane proteins: Tailored cell models out of microsomes. *Biochim. Biophys. Acta* **1838**, 1382–1388 (2013).
38. Wuu, J. J. & Swartz, J. R. High yield cell-free production of integral membrane proteins without refolding or detergents. *Biochim. Biophys. Acta* **1778**, 1237–1250 (2008).

39. Apponyi, M. A., Ozawa, K., Dixon, N. E. & Otting, G. Cell-free protein synthesis for analysis by NMR spectroscopy. *Methods Mol. Biol. Clifton NJ* **426**, 257–268 (2008).
40. Kim, R. G. & Choi, C. Y. Expression-independent consumption of substrates in cell-free expression system from *Escherichia coli*. *J. Biotechnol.* **84**, 27–32 (2000).
41. Kim, D. M. & Swartz, J. R. Prolonging cell-free protein synthesis by selective reagent additions. *Biotechnol. Prog.* **16**, 385–390 (2000).
42. Bayburt, T. H. & Sligar, S. G. Membrane protein assembly into Nanodiscs. *FEBS Lett* **584**, 1721–1727 (2010).
43. Yong, K. J. & Scott, D. J. Rapid directed evolution of stabilized proteins with cellular high-throughput encapsulation solubilization and screening (CHESS). *Biotechnol. Bioeng.* **112**, 438–446 (2015).
44. Van Duyne, G. D., Standaert, R. F., Karplus, P. A., Schreiber, S. L. & Clardy, J. Atomic structures of the human immunophilin FKBP-12 complexes with FK506 and rapamycin. *J. Mol. Biol.* **229**, 105–124 (1993).
45. Sreerama, N. & Woody, R. W. Estimation of protein secondary structure from circular dichroism spectra: comparison of CONTIN, SELCON, and CDSSTR methods with an expanded reference set. *Anal. Biochem.* **287**, 252–260 (2000).
46. Sreerama, N. & Woody, R. W. A self-consistent method for the analysis of protein secondary structure from circular dichroism. *Anal. Biochem.* **209**, 32–44 (1993).
47. Johnson, W. C. Analyzing protein circular dichroism spectra for accurate secondary structures. *Proteins* **35**, 307–312 (1999).
48. Provencher, S. W. & Glöckner, J. Estimation of globular protein secondary structure from circular dichroism. *Biochemistry (Mosc.)* **20**, 33–37 (1981).
49. Sreerama, N. & Woody, R. W. On the analysis of membrane protein circular dichroism spectra. *Protein Sci. Publ. Protein Soc* **13**, 100–112 (2004).
50. Scott, D. J., Kummer, L., Egloff, P., Bathgate, R. A. D. & Plückthun, A. Improving the apo-state detergent stability of NTS1 with CHESS for pharmacological and structural studies. *Biochim. Biophys. Acta* **1838**, 2817–2824 (2014).
51. Schanda, P. & Brutscher, B. Very Fast Two-Dimensional NMR Spectroscopy for Real-Time Investigation of Dynamic Events in Proteins on the Time Scale of Seconds. *J. Am. Chem. Soc.* **127**, 8014–8015 (2005).
52. Delaglio, F. *et al*. NMRPipe: a multidimensional spectral processing system based on UNIX pipes. *J. Biomol. NMR* **6**, 277–293 (1995).

Acknowledgements

This research was supported by National Health and Medical Research Council of Australia project grants [1081844] (RADB, DJS and PRG), the Victorian Government Operational Infrastructure Support Program. RADB is supported by an NHMRC Research Fellowship. PJS and FB are recipients of The University of Melbourne, Melbourne Research Scholarship.

Author Contributions

P.J.S., P.R.G., D.J.S. and R.A.D.B. conceived of and designed the study. P.J.S. conducted all cell free protein synthesis experiments. P.J.S. and F.B. acquired CD data and P.J.S. conducted ligand-binding studies; F.B. expressed and purified receptor from *E. coli*. P.J.S., F.B., P.R.G. acquired and processed NMR data. P.J.S. drafted the manuscript. All authors reviewed and edited the entire report and approved the final version for publication.

Additional Information

Supplementary information accompanies this paper at doi:10.1038/s41598-017-01227-z

Competing Interests: The authors declare that they have no competing interests.

Publisher's note: Springer Nature remains neutral with regard to jurisdictional claims in published maps and institutional affiliations.